UNITED NATIONS EDUCATIONAL, SCIENTIFIC AND CULTURAL ORGANIZATION
INTERNATIONAL ATOMIC ENERGY AGENCY
INTERNATIONAL CENTRE FOR THEORETICAL PHYSICS

SMR/917 - 10

**SECOND WORKSHOP ON**
**SCIENCE AND TECHNOLOGY OF THIN FILMS**

**( 11 - 29 March 1996 )**

---

" STM/AFM studies of kinetic scaling "

presented by:

J. KRIM
Northeastern University
Department of Physics
112 Dana Research Center
MA 02115 Boston
U.S.A.

---

These are preliminary lecture notes, intended only for distribution to participants.

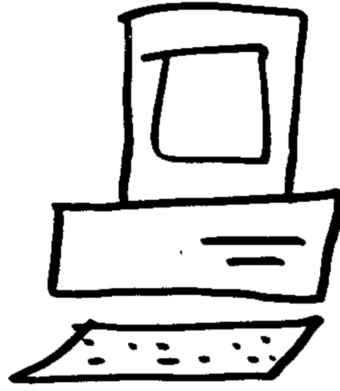

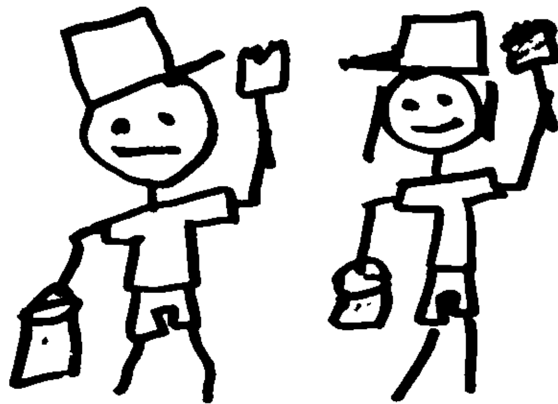

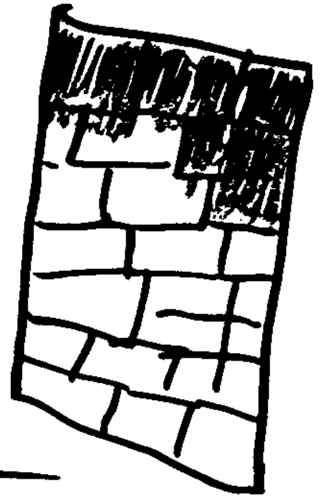

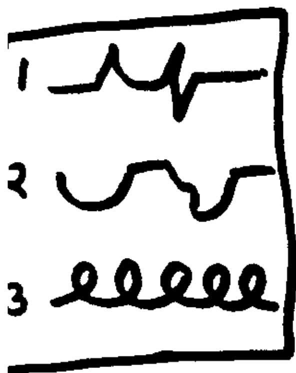
1
2
3

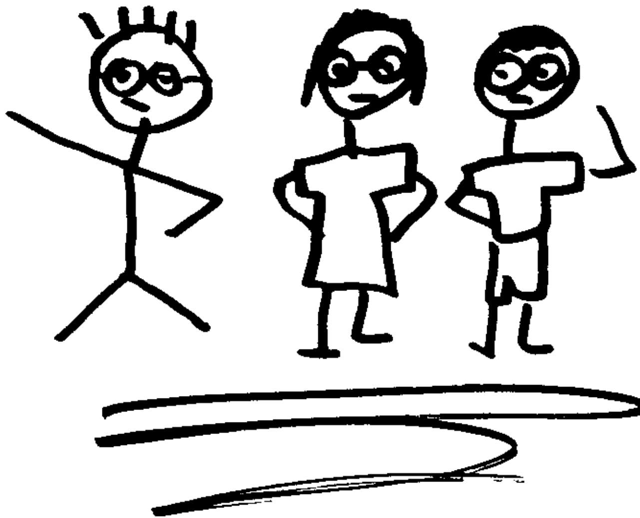

# "Kinetic Roughening"

- Surface grows "rougher" as film grows thicker

- Surface grows "rougher" as lateral distance increases, up to some cutoff.

Random Deposition without Surface Diffusion.

$\delta N \sim \sqrt{N}$

$N$: number deposited

$\sigma_{rms}(L) \sim L^{H}$ $H = 0$ $(\alpha = 0)$

$\sigma_{rms}(t) \sim t^{\beta}$ $\beta = 1/2$

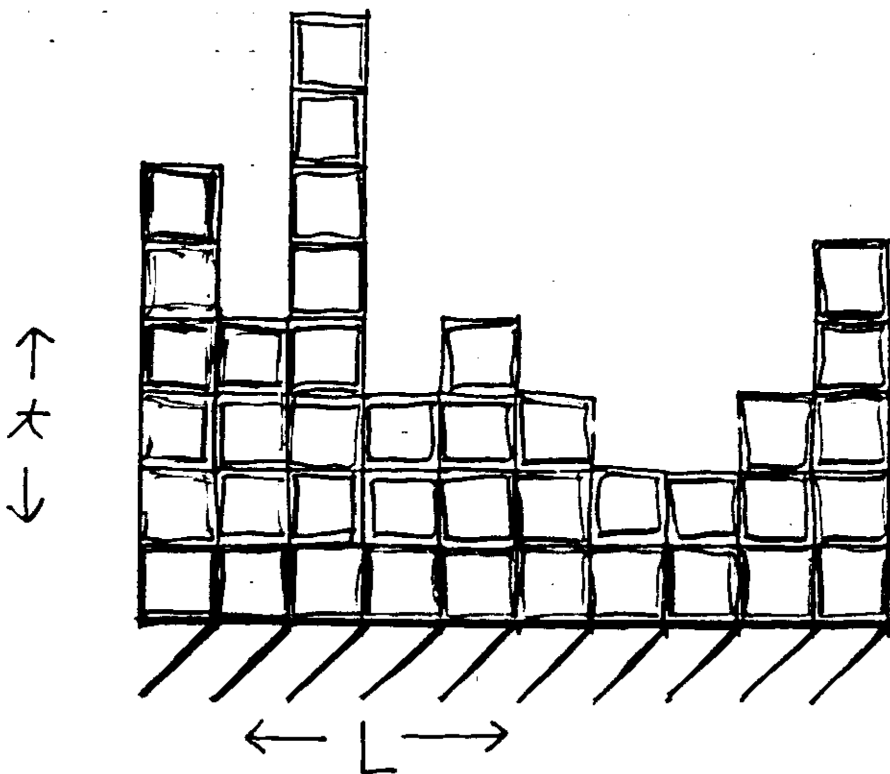


**With smoothing** $\beta < 1/2$

$H > 0$

| Model | Equation | $(\alpha, \beta)$<br>$(H, \beta)$ |
|---|---|---|
| Edwards – Wilkensen | $\frac{\delta h}{\delta t} = R_d + \eta + \nu \nabla^2 h$ | (0, 0) |
| KPZ | $\frac{\delta h}{\delta t} = R_d + \eta + \nu \nabla^2 h + \frac{\lambda}{2} (\nabla h)^2$ | ($\approx$ 0.35, 0.25) |
| "pure diffusion" | $\frac{\delta h}{\delta t} = R_d + \eta - \kappa (\nabla^4 h)$ | (1, 0.25) |
| "MBE" | $\frac{\delta h}{\delta t} = R_d + \eta - \kappa (\nabla^4 h) + \sigma \nabla^2 [\nabla h]^2$ | (0.67, 0.20) |
| "full diffusion" | $\frac{\delta h}{\delta t} = R_d + \eta +$ ~~$\nu \nabla^2 h$~~ $- \kappa (\nabla^4 h) +$ ~~$\sigma \nabla^2 [\nabla h]^2$~~ $+ \ldots$ | ! (1, 1/3)<br>(.8, 1) |

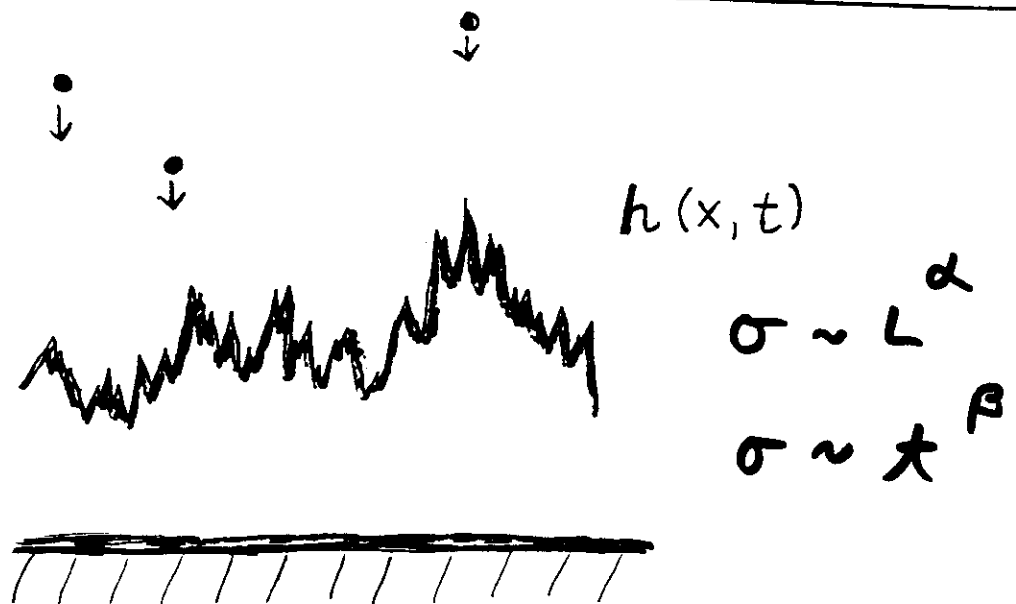

# DYNAMIC SCALING OF AN INTERFACE: $w(L,t) \sim L^H f\left(\frac{t}{L^{H/\beta}}\right)$

reference: F. Family, Physica A (1990)

"MBE"
$H = .7-1$
$\beta = 1/4 - 1/3$

$d = 2 = 1+1$

Random Deposition with Surface Diffusion: $\beta = 1/4$ $H = 1/2$ $(D = 1.5)$

Random
$H = 0$
$\beta = 1/2$

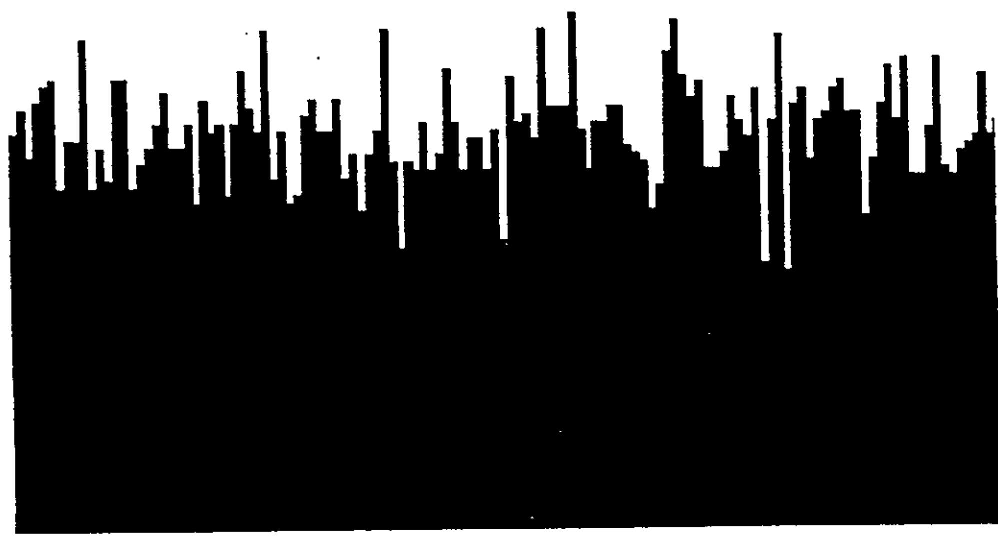

$d = 2$

Random Deposition: $\beta = 1/2$ $H = 0$ $(D = 2.0)$

KPZ
$H \cong .3$
$\beta = .25$

$d = 2$

Ballistic Deposition: $\beta \cong 1/3$ $H \cong 1/2$ $(D = 1.5)$

## 1988-1990 (3 papers)

## Selected Experimental Observations of Self-Affine Surfaces at Nanometer Length Scales

*X-Ray Reflectivity:* S.K. Sinha, E.B. Sirota, S. Garoff and H.B. Stanley, Phys. Rev. B **38**, 2297 (1988)

*Gas Adsorption:* P. Pfeifer, Y.J. Wu, M. W. Cole and J. Krim, Phys. Rev. Lett. **62**, 1997 (1989)

*Scanning Tunneling Microscopy:* M.W. Mitchell and D.A. Bonnell, J. Mater. Res. **5**, 2244 (1990)

## 1991-1993 (6 papers)

## Selected Experimental Observations of Self-Affine Scaling at Nanometer Length Scales

*X-ray reflectivity (in situ) and Gas Adsorption (in situ), silver film growth:* R. Chiarello, V. Panella, J. Krim and C. Thompson, Phys. Rev. Lett. **67**, 3408, (1991) $H = .7 \pm .1$; $\beta = .26 \pm .05$

*STM, graphite surface erosion:* E.A. Eklund, R. Bruinsma, J. Rudnick and R.S. Williams, Phys. Rev. Lett. **67**, 1759(1991)

*RHEED (in situ), iron film growth:* J. Chevrier, V. Le Thanh, R. Buys, and J. Derrien, Europhys. Lett. **16**, 737 (1991). $\beta = .25 - .32$

*Electron scattering (in situ), iron film growth:* Y.-L. He. H. N. Yang, T.M. Lu, and G.C. Wang, Phys. Rev. Lett. **69**, 3770 (1992). $H = .79 \pm .05$ $\beta = .22$

*STM (in situ), iron surface erosion:* J. Krim, I. Heyvaert, C. Van Haesendonck and Y. Bruynseraede, Phys. Rev. Lett. **70**, 57 (1993)

*X-ray reflectivity (in situ), gold film growth:* H. You, R.P. Chiarello, H.K. Kim, and K.G. Vandervoort, Phys. Rev. Lett. **70**, 2900 (1993).

$.8 < H, \alpha < 1.0$ $.2 < \beta < .4$

substrate tempertaure, $R_d$ the deposition rate, $P$ the pressure, $\theta$ the deposition angle with respect to the substrate normal, $h$ the film thickness, $\xi$ the correlation length, $\sigma$ the saturated rms width, $H$ the roughness exponent and $\beta$ the growth exponent.

| Substrate | $T_s$ K | $R_d$ nm/s | $P$ torr | $\theta$ deg. | $h$ nm | $\xi$ nm | $\sigma$ nm | $H$ | $\beta$ |
|---|---|---|---|---|---|---|---|---|---|
| | | | | **Ag** | | | | | |
| quartz[45] | 80 | 0.05 | $10^{-8}$ | 5 | 110 | 145 | 0.85 | 0.46 | |
| quartz[68] | 80 | 0.03 | $10^{-7}$ | 5 | 45-250 | | | fractal | |
| Si[49] | 300 | 0.03 | $10^{-7}$ | 0 | 10-150 | < 100 | 0.5–3.5 | 0.70 | 0.26 |
| Ag(111)[71,72] | 300 | 0.004 | $10^{-10}$ | 0 | 0.15-6 | | 0.1-0.8 | 1 | |
| quartz[73] | 300 | 0.03 | $10^{-8}$ | 0 | 30-700 | 15-60 | 2.2-6.0 | 0.82 | 0.29 |
| | | | | **Au** | | | | | |
| Si(111)[74] | 220 | 0.05 | $10^{-2}$ | | 350 | 200 | 3 | 0.42 | |
| Si(111)[74] | 220 | 0.05 | $10^{-2}$ | | 7-270 | | 0.5-2.5 | | 0.42 |
| glass[4] | 300 | | $10^{-1}$ | 0 | 50 | | | 0.74 | |
| glass[62] | 300 | 30 | $10^{-4}$ | 2-25 | 30-850 | ≈ 40 | 0.7-2.6 | 0.89 | 0.41 |
| Si(111)[74] | 300 | 0.05 | $10^{-2}$ | | 10-120 | | 0.6-2.0 | | 0.40 |
| quartz[45] | 500 | 0.05 | $10^{-9}$ | 0 | 150 | 330 | 2.2 | 0.95 | |
| quartz[45] | 500 | 0.05 | $10^{-9}$ | 0 | 150 | | | not fractal | |
| | | | | **Cu** | | | | | |
| Cu(100)[15] | 160 | 0.001 | $10^{-9}$ | * | 0.5-7.5 | | 0.15-0.3 | 1 | 0.26 |
| Cu(100)[15] | 160 | 0.001 | $10^{-9}$ | * | 2.35 | 2.2 | 0.22 | | |
| Cu(100)[15] | 200 | 0.001 | $10^{-9}$ | * | 0.5-11 | | 0.1-0.8 | 1 | 0.56 |
| Cu(100)[15] | 200 | 0.001 | $10^{-9}$ | * | 7.2 | 10.6 | 0.72 | | |
| Cu[75] | 300 | 8.3 | | | 500-30000 | $10^3$ | 100-700 | 0.87 | 0.45 |
| | | | | **Si** | | | | | |
| Si[67] | 573 | 0.01 | | | 5-30 | | 0.2-1.2 | | 1 |
| | | | | **Fe** | | | | | |
| Si(111)[76] | 323 | 0.01 | $10^{-10}$ | | 0.2-75 | | 0.25-8.5 | | 0.22-0.3 |
| Fe(001)[6] | 343 | 0.01 | | | 0.5-0.31 | ≈ 1.4 | 0.11-0.16 | 0.79 | 0.22 |
| | | | | **AlCu and AlSi** | | | | | |
| AlCu/Si[47] | 473 | | | | 468 | 110 | 1.8 | 0.7 | |
| AlSi/Si[47] | 473 | | | | 600 | 400 | 4.2 | 1 | |

| Substrate | $T_s$ K | $R_d$ nm/s | $P$ torr | $\theta$ deg. | $h$ nm | $\xi$ nm | $\sigma$ nm | $H$ | $\beta$ |
|---|---|---|---|---|---|---|---|---|---|
| | | | | **InP** | | | | | |
| InP(1000)[77] | 773 | 0.01-0.05 | | | 0.1-100 | | 0.05-0.1 | | 0.2 |
| | | | | **NbN** | | | | | |
| sapphire[66] | 573 | 4 | | | 20-500 | | 0.5-1.5 | | 0.27 |
| | | | | **CuCl** | | | | | |
| $CaF_2$(111)[78] | 353, 383.04 | | | | 6-40 | ≈ 200 | ≈ 20 | 0.84 | |
| | | | | **$CH_{1.3}$ Polymer** | | | | | |
| Si[79] | 318 | 0.55 | | | 30-20,000 | 20-2000 | 1-100 | 0.90 | 0.7 |
| Si[79] | 318 | 0.41 | | | 500-20,000 | $10^3$ | 1-100 | 0.95 | 0.9 |
| Si[79] | 318 | 0.27 | | | 1-70, $\times 10^3 10^3$ | | 1-100 | 1.1 | 1.0 |
| Si[79] | 318 | 0.22 | | | 1-8, $\times 10^4$ | | 0.6-2 | | 0.27 |

*angle varied

Scanning Probe Microscopes record $z(x,y)$ in an array.

100 x 100, 400 x 400, etc.

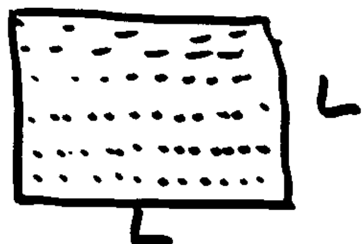


Methods for obtaining $H$:

- Multiple scans varying $L$, then
  $\sigma \sim L^H$
- Single image analysis
  $\sigma \sim L^H$, subdividing image into smaller portions
  $$g(R) = \langle [z(x',y') - z(x,y)]^2 \rangle \propto R^{2H}$$
- Fourier power spectrum
  $$\sum_{k=0}^{\infty} A_k e^{ikx}$$
- "Loop" Dimensions

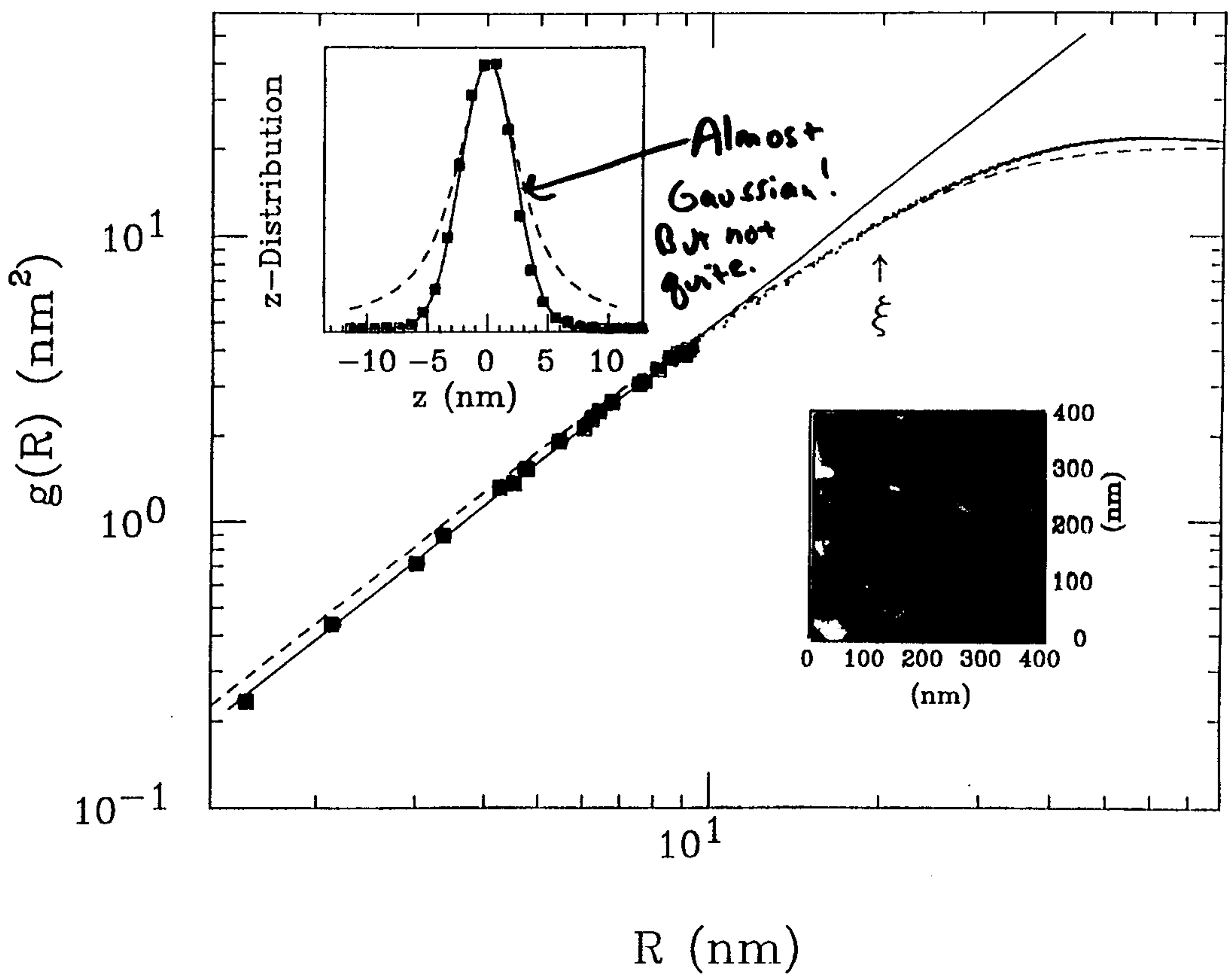

g(R) (nm²)
10⁻¹
10⁰
10¹
R (nm)
z-Distribution
-10 -5 0 5 10
z (nm)
Almost Gaussian! But not quite.
ξ
0 100 200 300 400
(nm)

4 x $10^3$

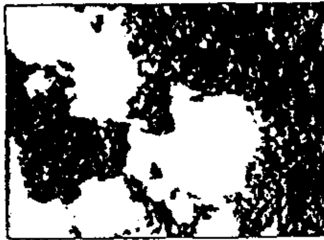


6.5 x $10^4$

1.7 x $10^7$

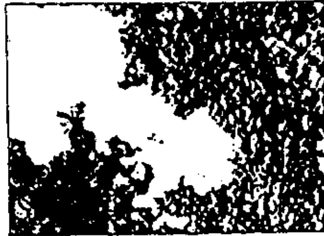


1 x $10^0$

R. Voss, in "The Science of Fractal Images"

200 nm

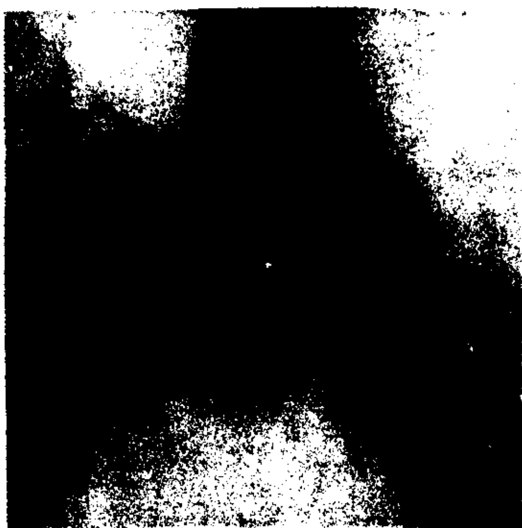

600 nm

50 nm

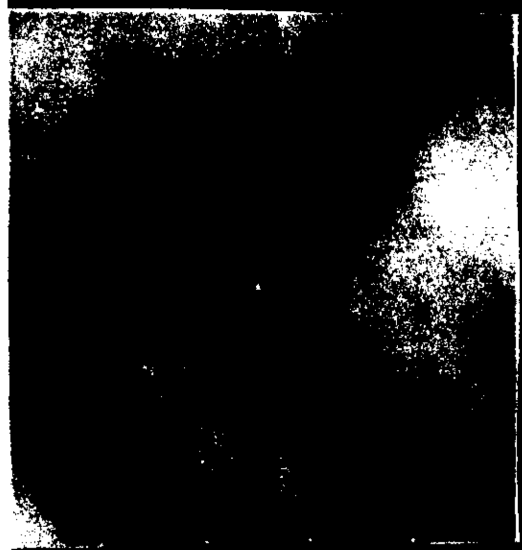

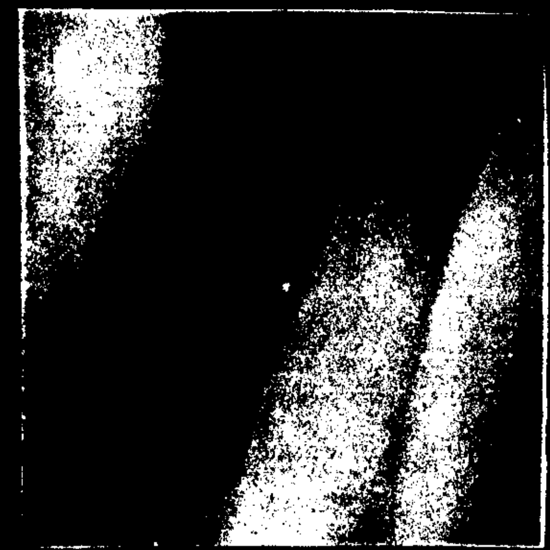

2000 nm

J. Krim, I. Heyvaert, C. Van Haesendonck & Y. Bruynseraede (preprint) PRL Jan '93 70, 57 (1993)

"test gold sample"

# Gold Film "Test Sample"

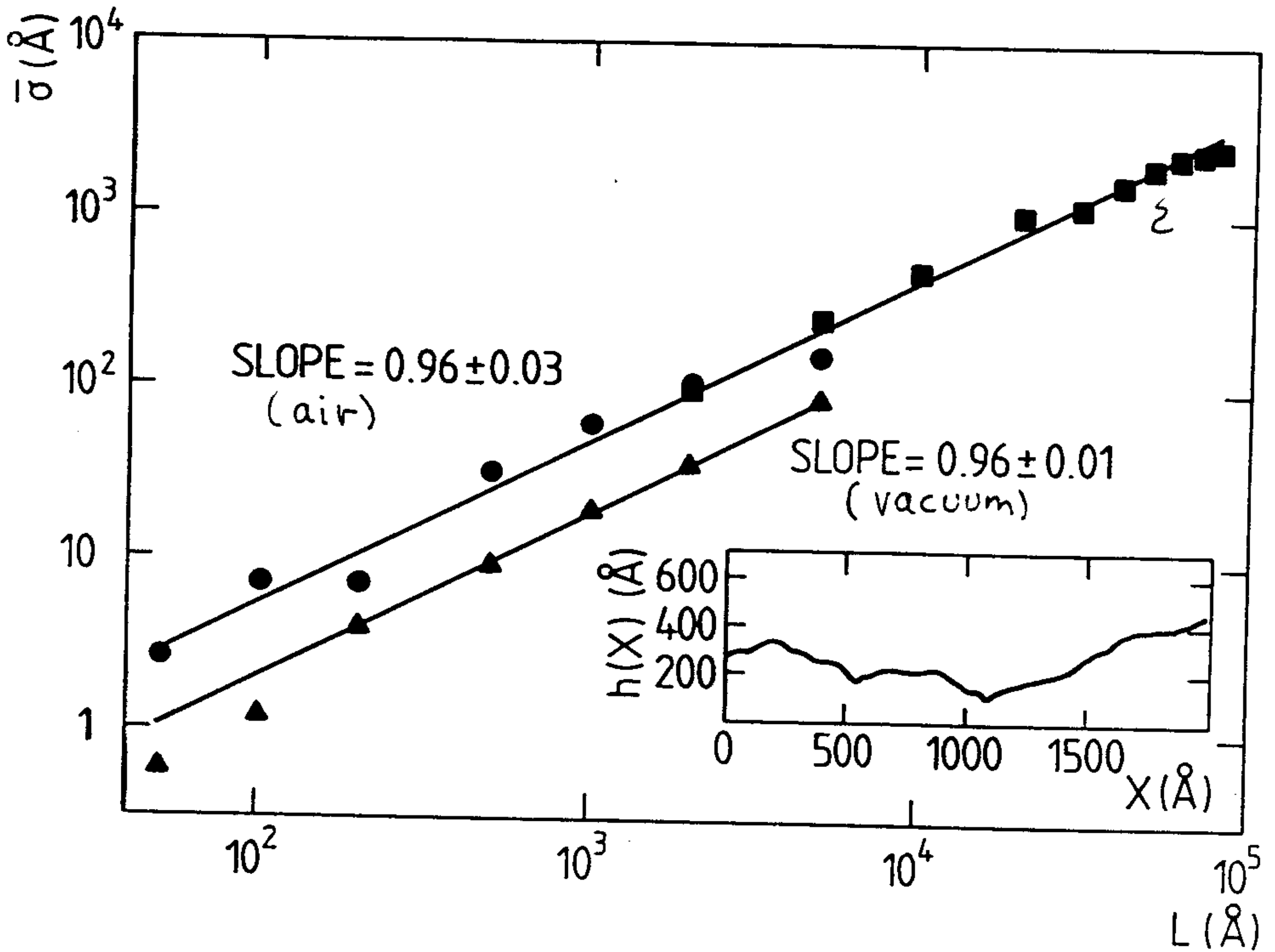


STM : $\sigma \sim L^H$ $H = 0.96 \pm 0.03$ ($D = 2.04$)

Adsorption : $H = .97 \pm 0.1$ (neglecting surface tension)

$H = .49 \pm 0.1$ (including surface tension)

($O_2$ & $N_2$ Adsorption identical)

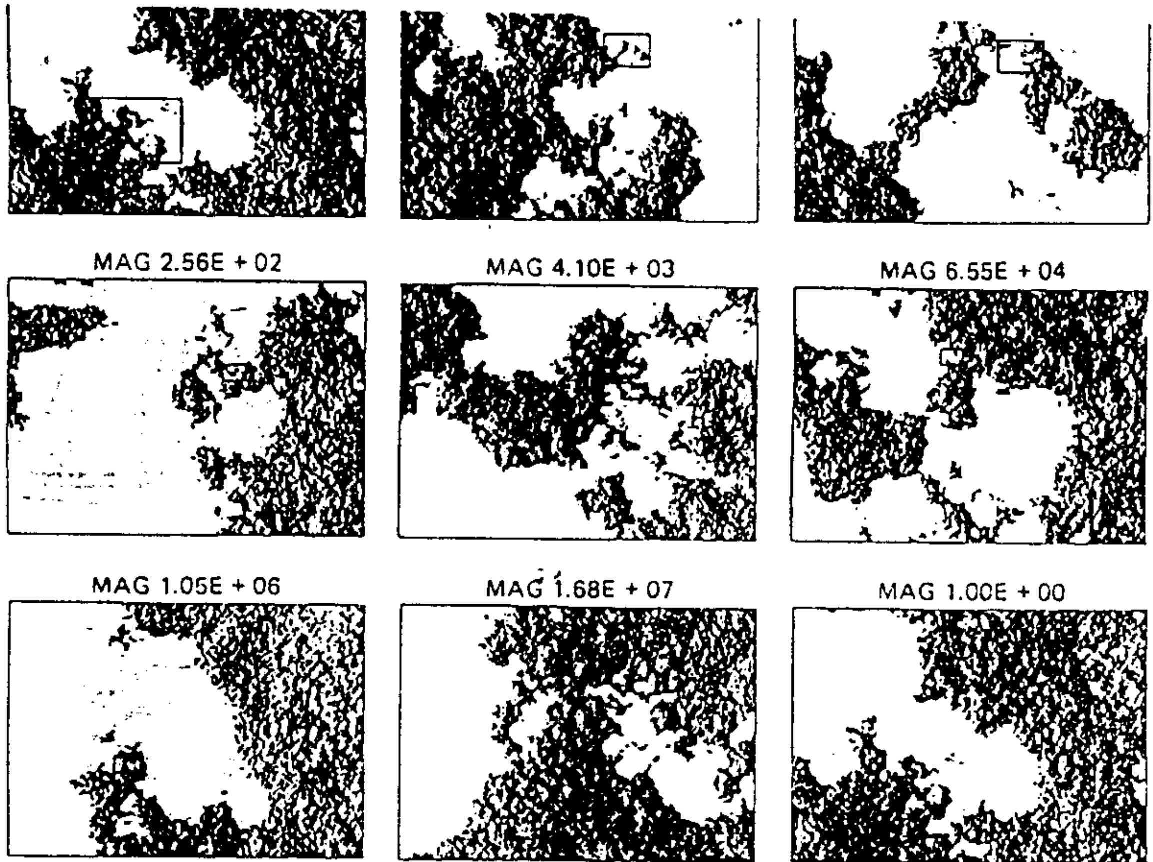


**Fig. 1.1:** Zoom sequence of the coastline of a statistically self-similar fractal landscape $D = 2.2$. Each succeeding picture shows a blowup of the framed portion of the previous image. As the surface is magnified, a small portion looks similar to (but not exactly the same as) a larger portion. The total magnification corresponds to 16 million. (Copied from R.F. Voss, in "The Science of Fractal Images", H-O Peitgen and D. Saupe, eds. (Springer-Verlag, New York, 1988), page 23)

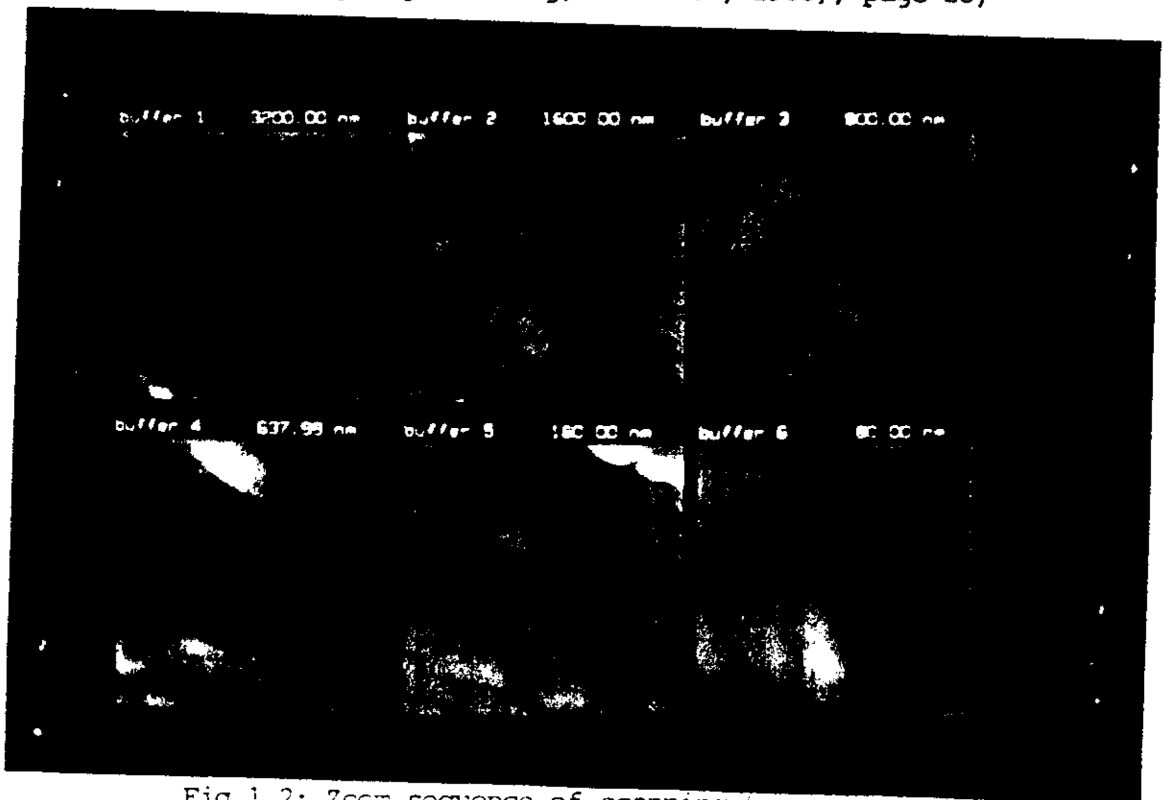


Fig.1.2: Zoom sequence of scanning tunneling microscope

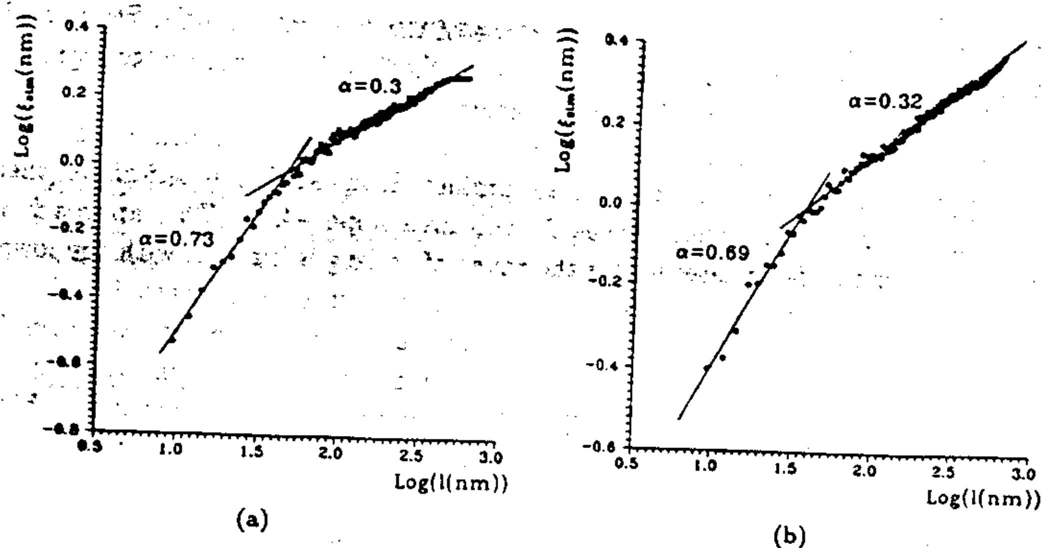


Fig. 9. Rms width $\xi$ vs scale length obtained from a single STM image recorded in a gold film evaporated onto a smooth glass substrate for both the (a) $x$ direction and the (b) $y$ direction. The slopes of the solid lines fit to the $x$ direction yield roughness exponents 0.3 for (horizontal) length scales greater than $\approx 40$ nm, and 0.89 for length scales less than $\approx 40$ nm (see text). This figure is reproduced from Salvarezza *et al.*, Ref. 62.

The desirability of a given analysis approach depends on the range of scaling of the particular sample *viz a viz* the scan size analyzed, the grid density of the topograph, and the number of topographs available for averaging. STM cannot be employed for nonconducting surfaces, in which case AFM can be used. The tip-surface distance in the non-contact mode of AFM imaging is however greater than that for STM, with a resulting loss in resolution.

In practice, the determination of $\beta$ is more problematic for the scanning probe microscopies than the determination of $H$. This is because the rms width does not effectively saturate until the lateral scan size exceeds many times the sample correlation length, and a scan head capable of probing the relevant length scale may not readily be available. If the saturation value for $\sigma$ can be established, then $\beta$ can be directly obtained from its dependence on film thickness.

### 3.6. *Electron microscopy*

Scanning Electron Microscopy (SEM) is a technique which has long been employed for sub-micron characterizations of surface topology. It involves scanning a focused electron beam (primary energy typically 2–10 keV) over the surface while simultaneously detecting the emitted electrons. The intensity of the emitted signal is associated with variations on the local surface topology of the sample. Under ideal circumstances, the electron beam can be focused to as little as 1 nm.[54]

SEM is generally employed for qualitative, rather than quantitative characterizations of surface morphology, due to the complex nature of the dependence of electron yield on surface chemical and topological properties. It nonetheless has

$d = 2 + 1 = 3$ spacial dimensions

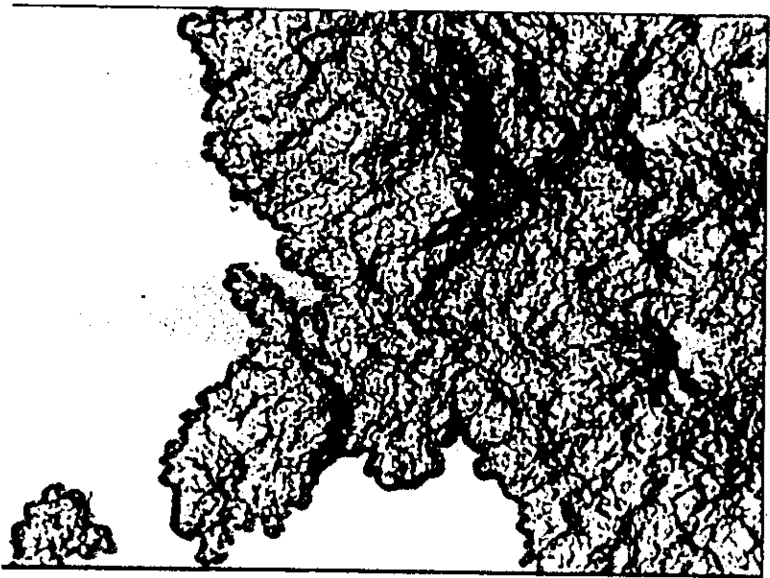

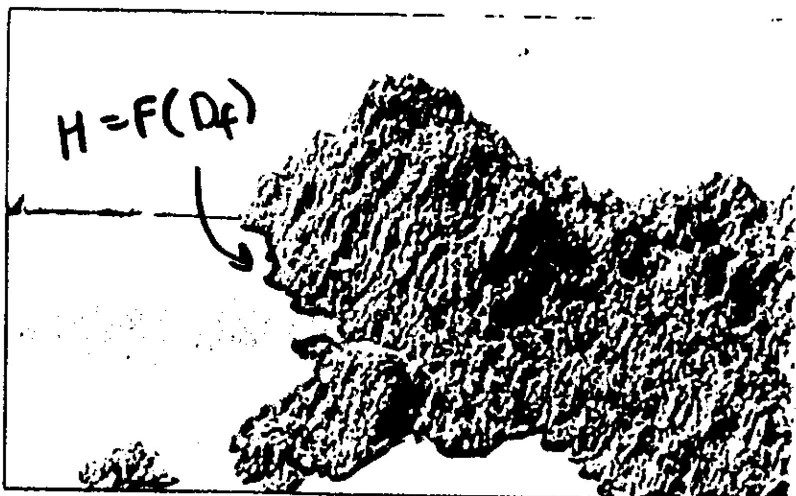


a

# Ag / quartz @ 300K   H = .82

(D = 2.0 for QCM)

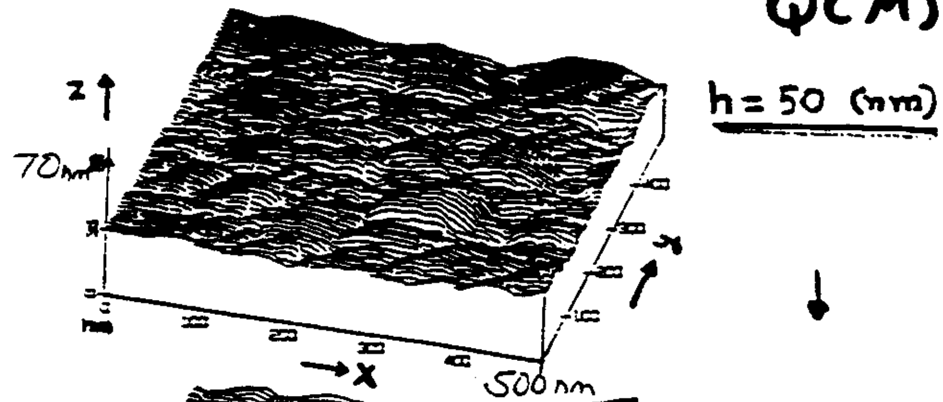


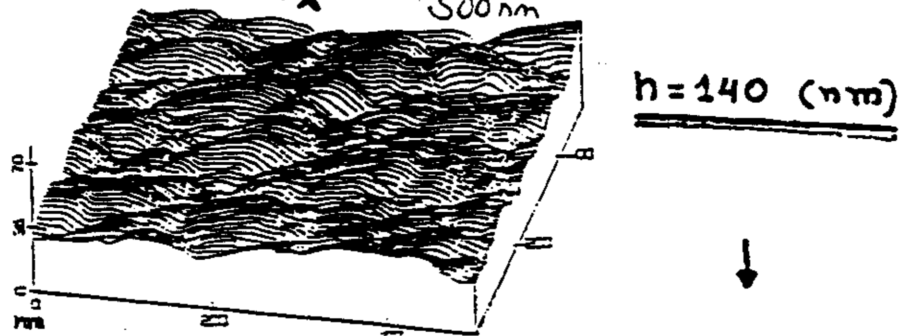


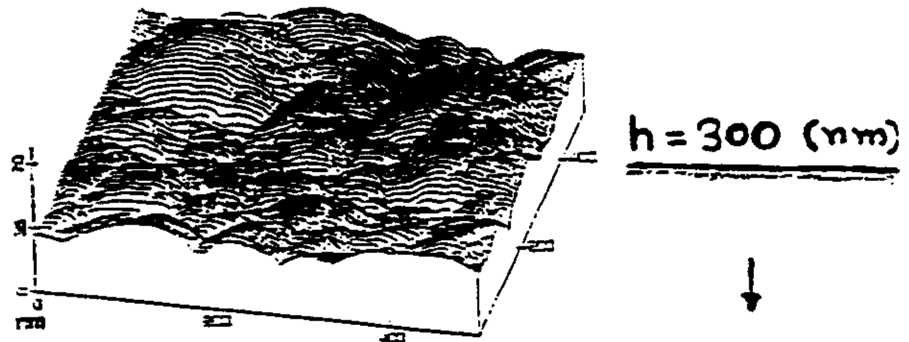


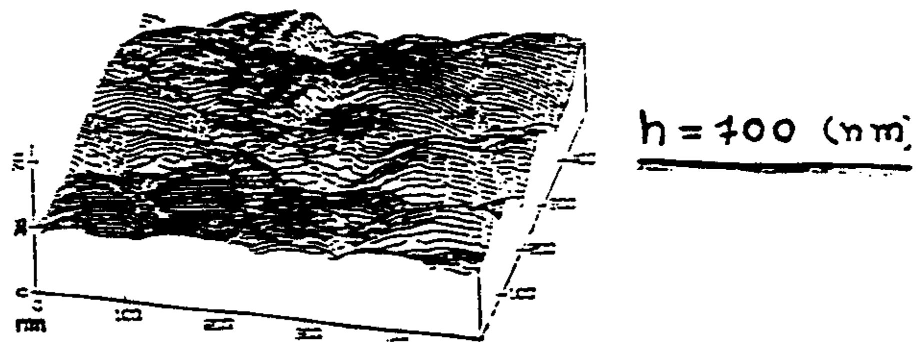


G. Palasantzas & J. Krim PRL Dec '94 (STM)

Thompson et al. PRB '94 (XRR)

STM Data recorded on Silver deposited at room temp. (Krim et al PRL '91)

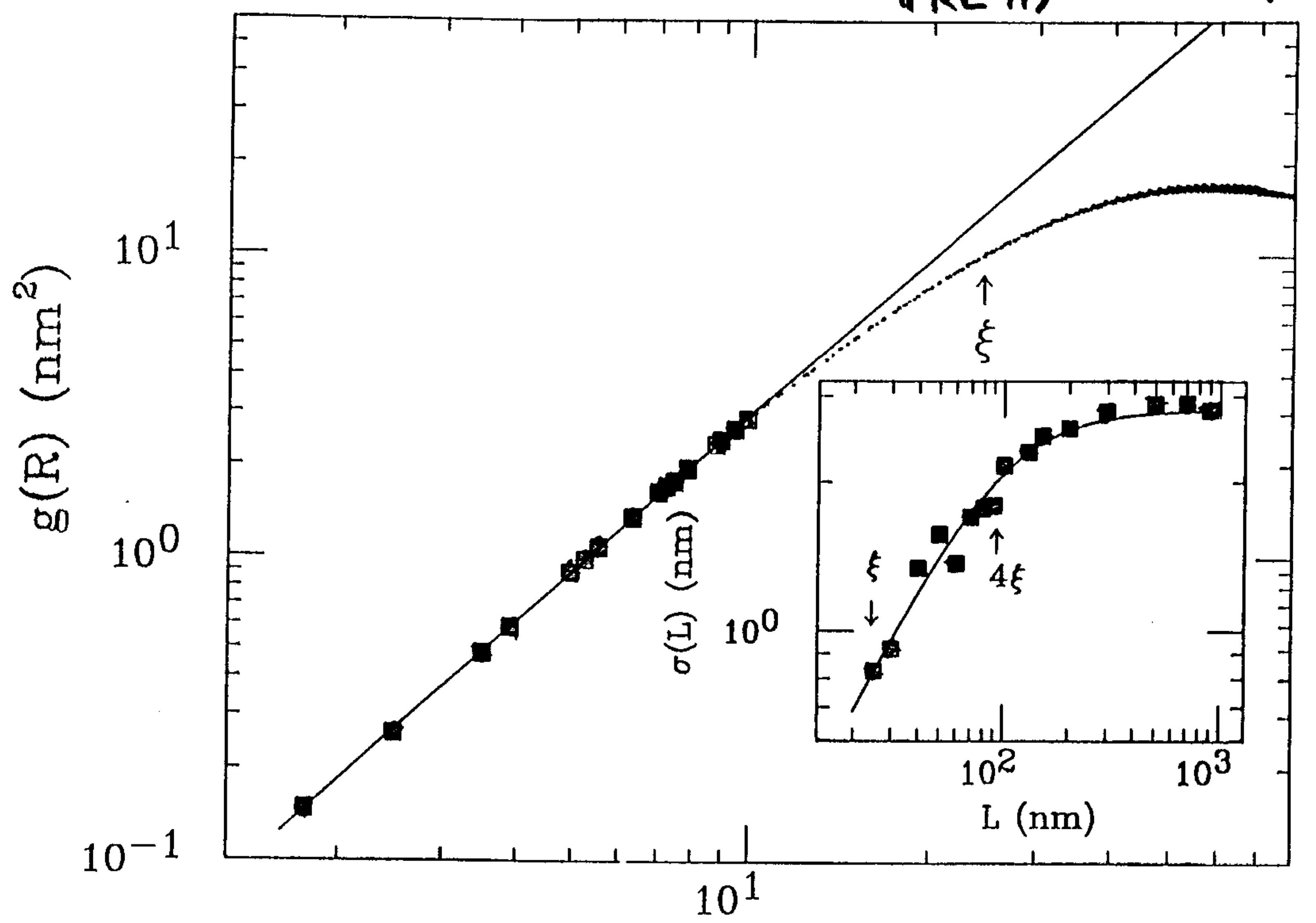


$g(R) = \langle [z(R) - z(0)]^2 \rangle \sim R^{2H}$

$\sigma \sim L^{H}$

Diffuse X-ray reflectivity from silver films prepared at 300 K.

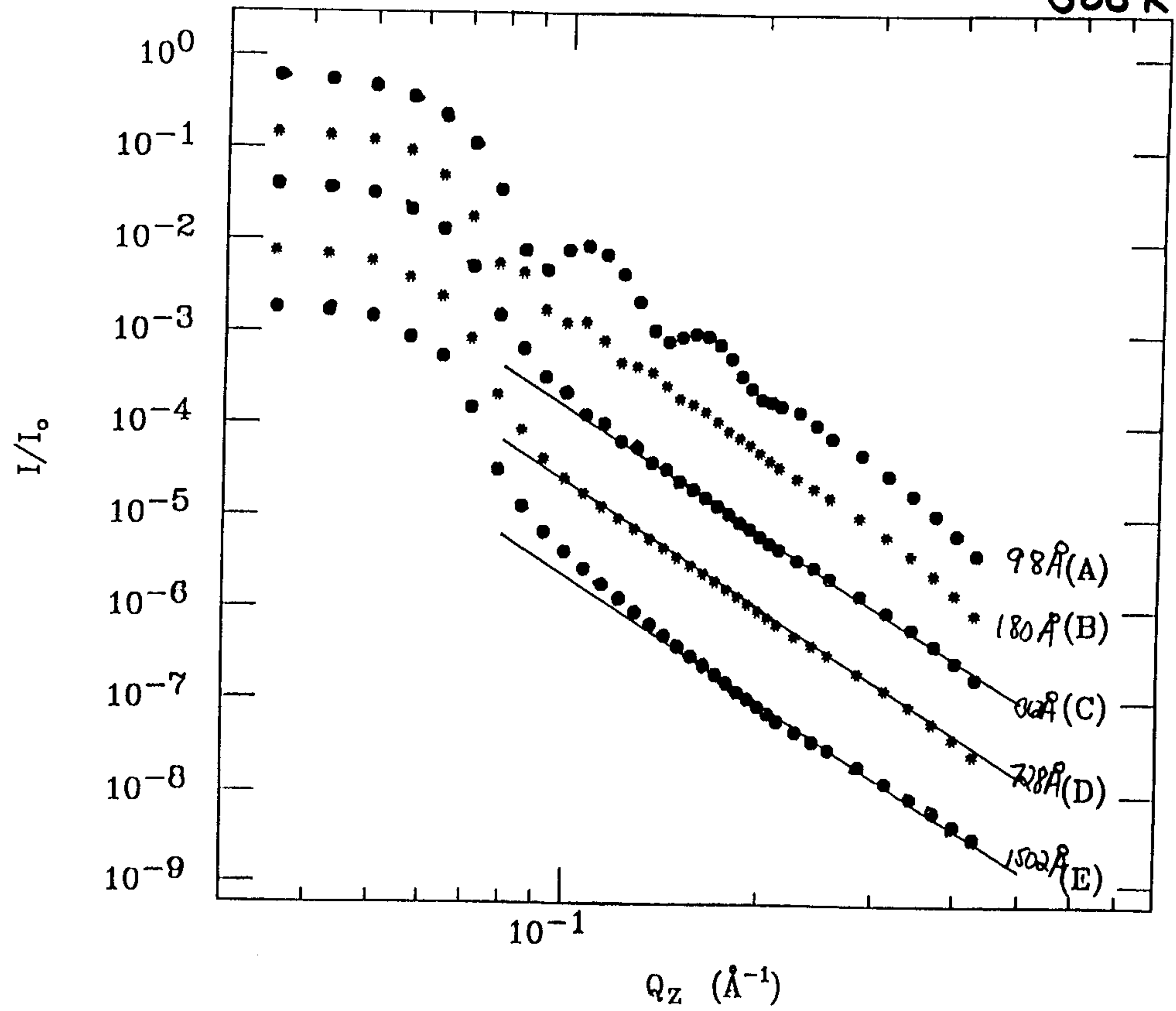

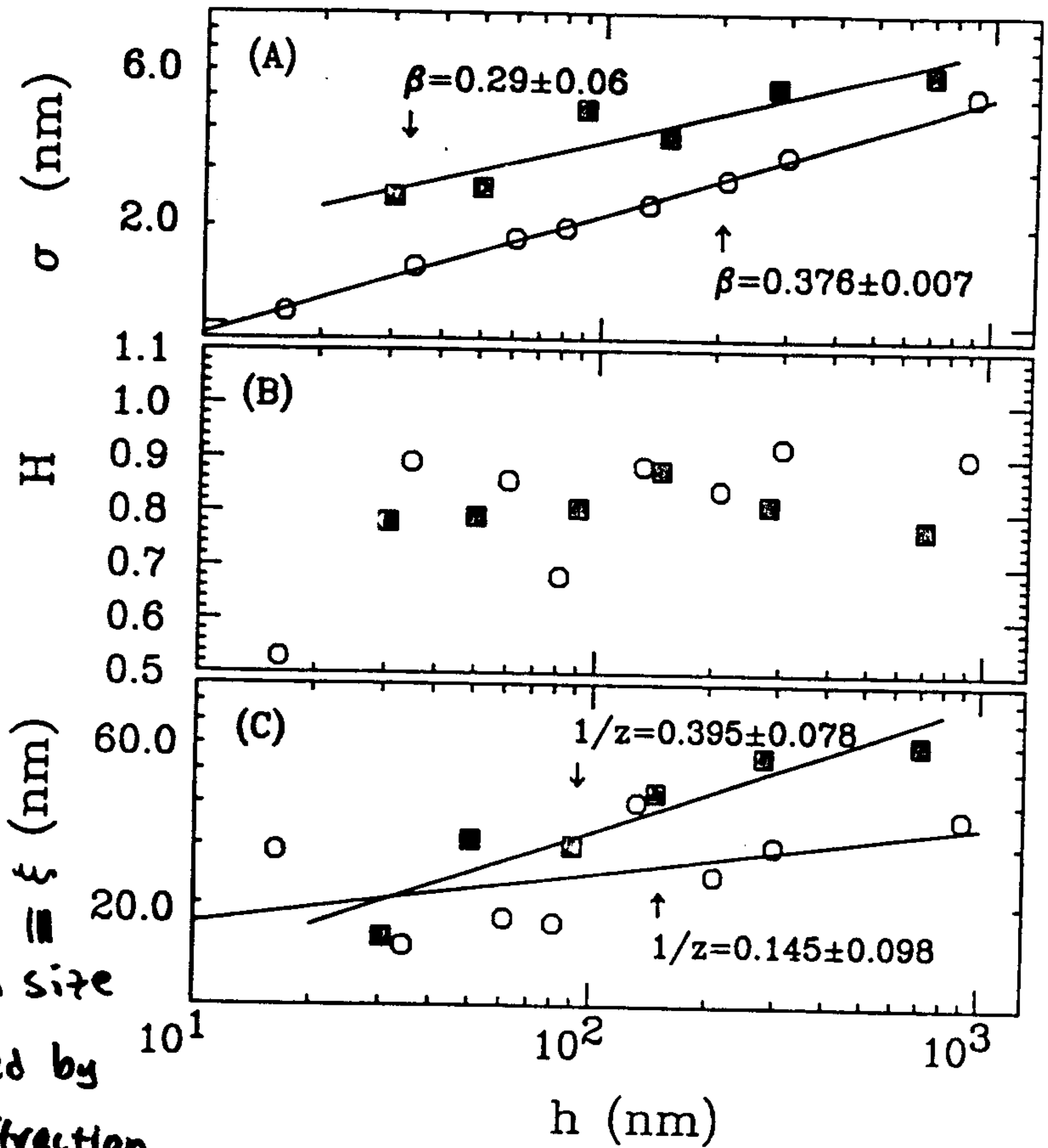


≡ grain size as measured by X-ray diffraction

$$z = \frac{H}{\beta} \text{ satisfied}$$

100 nm →

30 nm

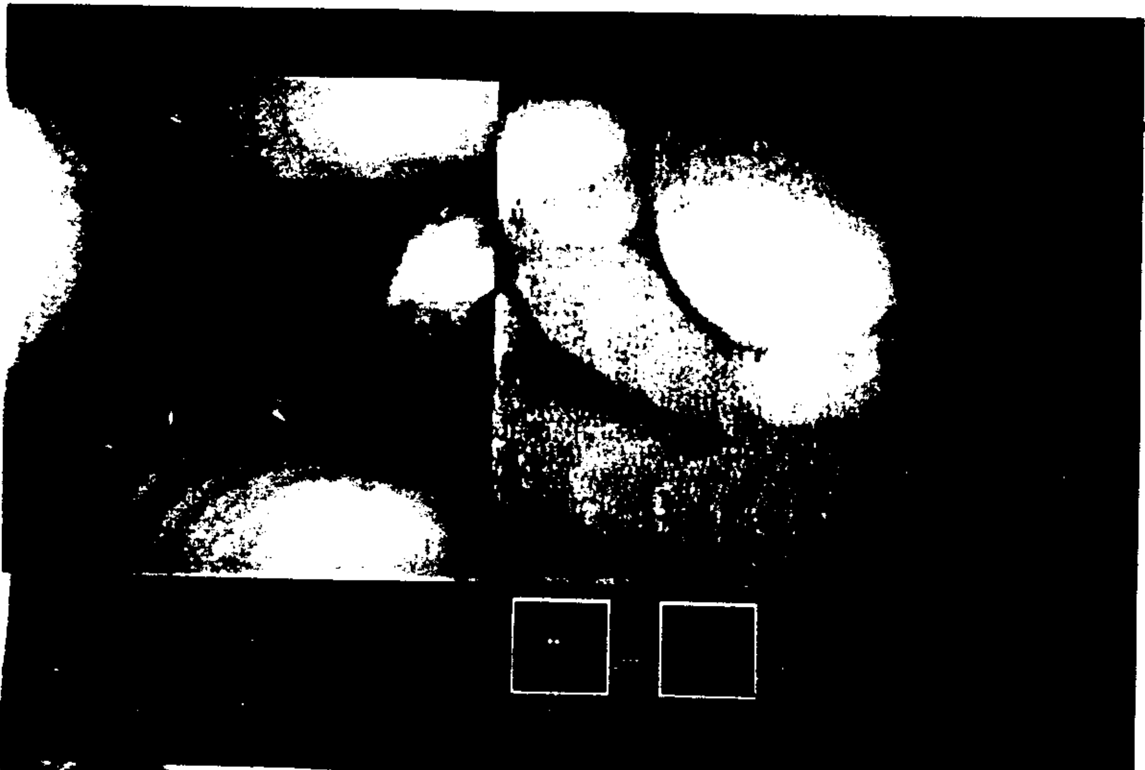

200 nm ↔

10 nm

500 nm →

200 nm

200 nm ↔

200 nm

100 nm →

3 nm

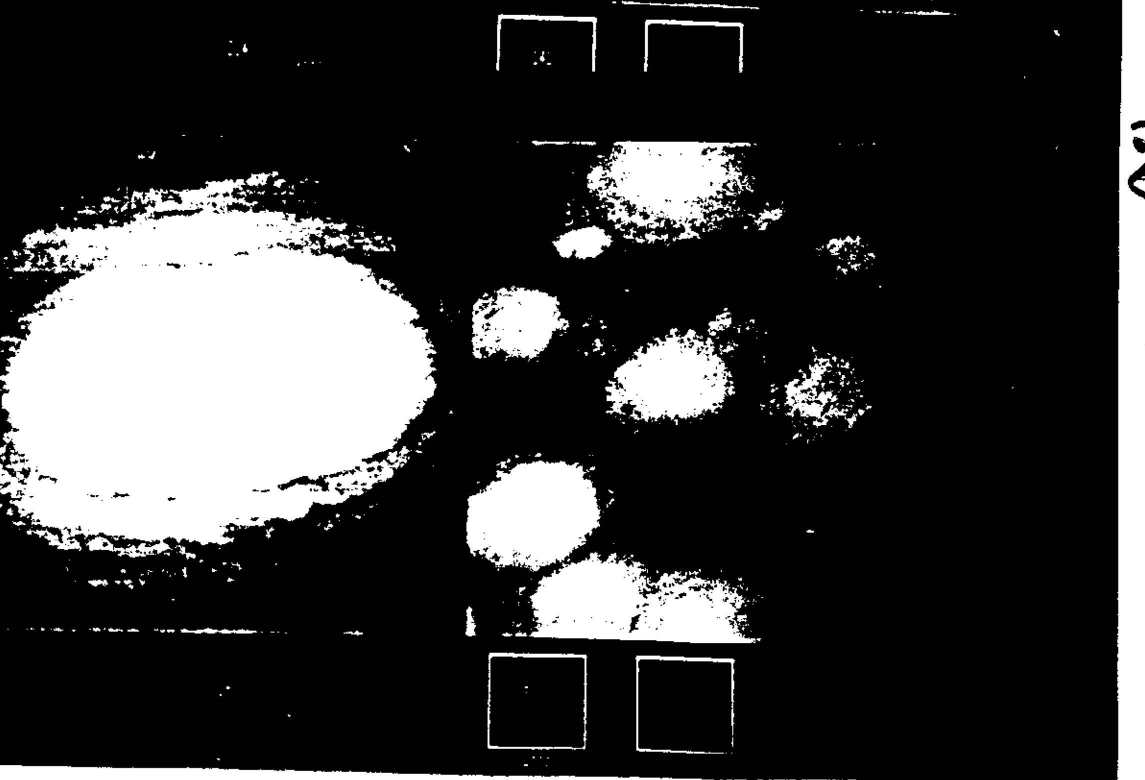

200 nm ↔

10 nm

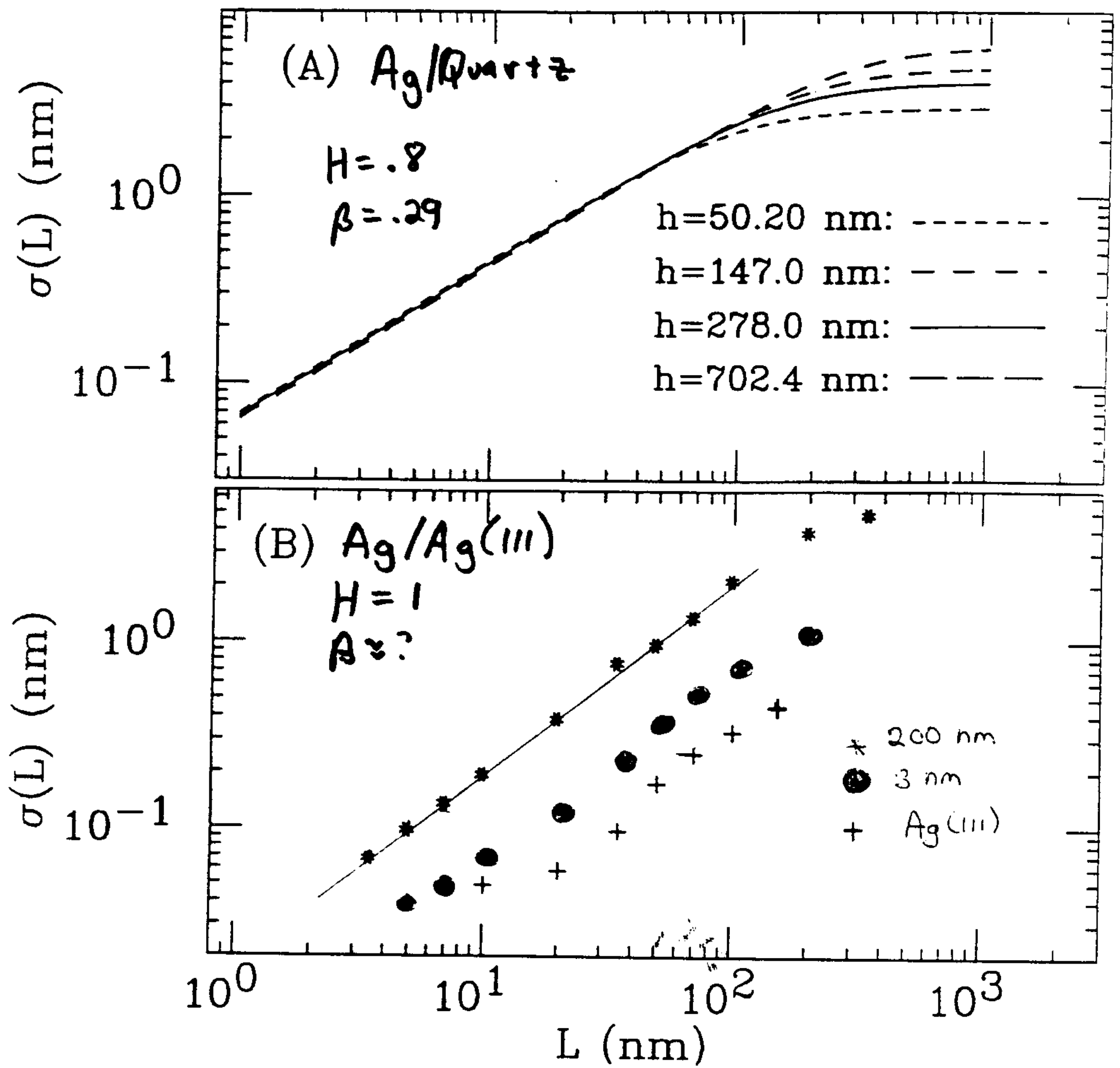
(A) Ag/Quartz
H=.8
β=.29
h=50.20 nm:
h=147.0 nm:
h=278.0 nm:
h=702.4 nm:
σ(L) (nm)
(B) Ag/Ag(111)
H=1
β≈?
200 nm
3 nm
Ag(111)
σ(L) (nm)
L (nm)

produced dramatic evidence for scale invariance in a variety of samples, demonstrated by images which appear identical regardless of magnification. The most well-known examples of these are the carbon cauliflower-like structures which have been reported by Messier *et al.*[64]

Quantitative information from SEM can be obtained by studying the cross-section and internal structure of the films if they can be sectioned and/or ion-milled. Fractal scaling properties of specimens are usually determined by polishing, in stages, the surface in the in-plane direction so as to reveal 'islands', and their associated self-similar 'coastlines'. The roughness exponent $H$ is inferred directly from the fractal dimension of these coastlines. Fractal scaling properties can also be probed in a nondestructive fashion by means of a stereoscopic SEM method.[65]

Transmission Electron Microscopy (TEM) involves the use of high energy electrons ($> 50\,\mathrm{keV}$), which are diffracted as they pass through a thin sample and are then focused into an image consisting of a two-dimensional projection of the sample structure. Under ideal circumstances, the image resolution can be as little as 0.2–0.3 nm. Layer structures documenting the evolution of surface roughness can be observed in sufficiently thin ($\approx 100\,\mathrm{nm}$ or less) vertical film slices, by 'marking' the film at regular intervals through deposition of a contrasting element (Fig. 10).[66,67]

β= .27

**Fig. 10.** Sequential cross-section TEM micrograph of a multilayer film which has been thinned to ≈ 40 nm for electron transparency. The multilayer is comprised of 101 layers of AlN which are 2 nm thick, alternating with 100 layers of NbN which are 3 nm thick. This figure is reproduced from Miller *et al.*, Ref. 66.

AlN /NbN multilayers / sapphire

/Cu(100) Electrodeposition
=1 $\beta = .26$

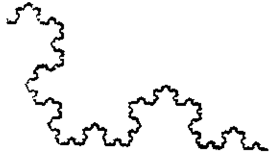

D = 1.262 (upper surface) and a self-affine
produced from Panella and Krim, Ref. 68.

rm,

$/L^{H/\beta})$ (1)

$) \propto t^{\beta}$ for $t/L^{H/\beta} \to 0$. Implicit in
with time as $\xi \propto t^{1/z}$, where $z = H/\beta$
nt. Figure 3 depicts AFM images of
r films which are well-described by
of the surface, the vertical and hor-
caled in accordance with the spatial
the quantitative analysis of the sur-

nents commonly derive from partial
al expansions in the derivatives of a
cribing film growth at a mesoscopic
very well-known example of this ap-
does not conserve particle number,
orption and/or vacancy formation,
ace relaxation mechanisms. Numer-
sequently been proposed,[10] since in
relaxation mechanism is surface dif-
orption being quite negligible. One
n Epitaxy" (MBE), where material
gle crystal at sufficiently high tem-
epitaxial relation to the substrate.

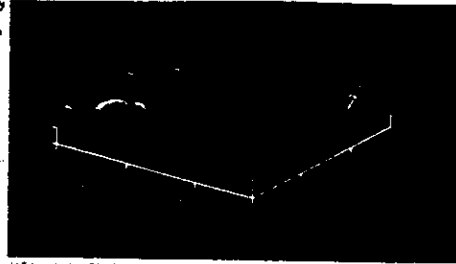

5 min

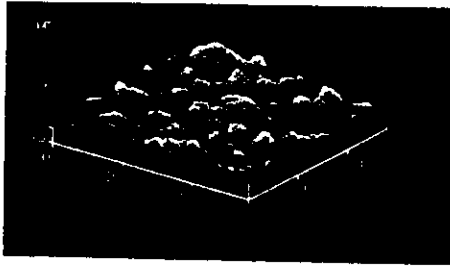

30min

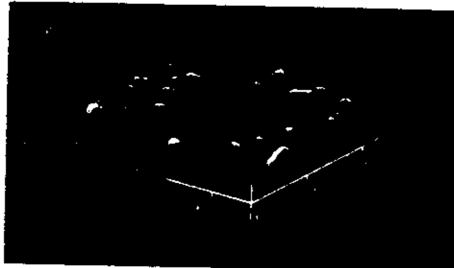

60min

**Fig. 3.** AFM images of copper surfaces electrodeposited in an acid sulfate solution with an electric current density of 2.4 A/dm$^2$ for electrodeposition times of (a) 5, (b) 30, and (c) 60 min. To demonstrate the scaling behavior of the surface, the vertical and horizontal dimensions are anisotropically scaled in accordance with the spatial and temporal scaling deduced from the quantitative analysis of the surface height correlations. This figure is reproduced from Iwamoto *et al.*, Ref. 75.

Conservative models have thus also come to be known as "MBE" models, and they predict distinctly different values for the scaling exponents. Measurements of $H$, $\beta$ and $z$ are therefore expected to shed light on the atomic-scale origins of particular film morphologies.

Table 1 lists asymptotic values for the scaling exponents associated with growth on a two-dimensional substrate, for selected continuum equations. We note that the theoretical treatment of MBE growth is currently the subject of very lively debate, and the last two equations are listed as representative only. The values quoted for the first and third equations are analytically exact,[21,22] while the values quoted for

polymer/Si
H ≈ 1
β ≈ .27, 1
↑ ↑
slow fast
Rd Rd

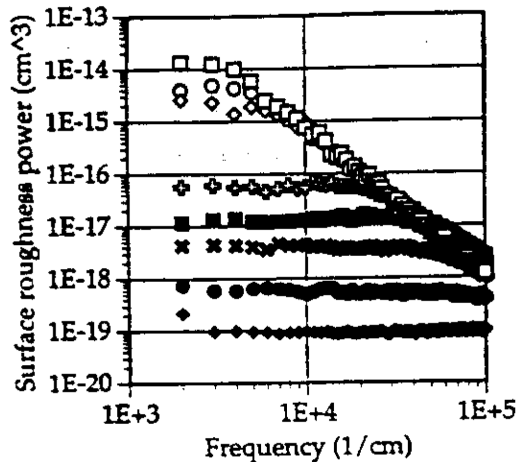


Fig. 15. Evolution of the surface roughness power spectra with increasing film thickness for plasma polymer films deposited at 0.55 nm/s. 19.7 μm (open squares), 11.1 μm (open circles), 8.5 μm (open diamonds), 1.1 μm (+), 0.53 μm (filled squares), 0.28 μm (x), 0.14 μm (filled circles), 0.07 μm (filled diamonds). This figure is reproduced from Collins *et al.*, Ref. 79.

and $z = 1$ for 1000–70,000 nm thick films deposited at 0.27 nm/s, and $\beta \approx 0.27$ for 10,000–80,000 nm thick films deposited at 0.22 nm/s. Collins *et al.* argued that scaling theories of kinetic growth could be applicable to cases of polymer growth, despite the fact that the deposited particles were intertwined, and interpreted their results as supportive of conservative growth models.

## 5. Erosion and Other Studies

The sub-micron topology of a surface produced by ion bombardment or erosion has received far less theoretical attention than that of a vapor-deposited film.[80] The scaling theories applicable to nonequilibrium film growth might however be applicable to cases of erosion, if no material is redeposited onto the surface during the erosion process.[81] If so, the topography of a film deposited onto an initially smooth substrate would be quite similar to that of an initially smooth surface which is subjected to ion-bombardment: a self-affine fractal surface is expected to develop and its rms width should exhibit a power law dependence on time. Experimental reports of sub-micron scaling phenomena for cases of surface erosion are listed in this section, and summarized in Table 3. We also mention here of a case involving the evolution of surface roughness due to time-dependent rearrangement of material at the surface rather than its addition or removal.

### 5.1. *Ion-beam erosion*

#### 5.1.1. *Graphite*

*1991:* Eklund *et al.*,[82] exposed the (0001) surface of highly-oriented pyrolytic graphite to 5 keV $Ar^+$ ions at an angle of 60° with respect to substrate normal.

$H = 0.50$ $D = 2.50$

$H = 0.80$ $D = 2.20$

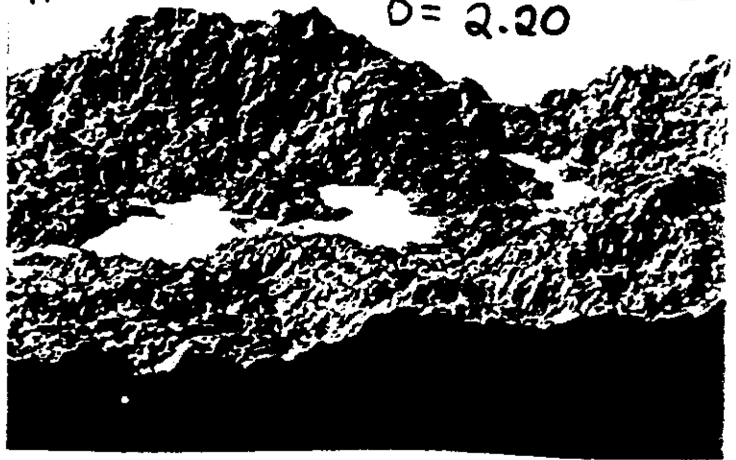

B. Mandelbrot, "The Fractal Geometry of Nature"

$L = 2000$ Å
vertical scale: 23 Å

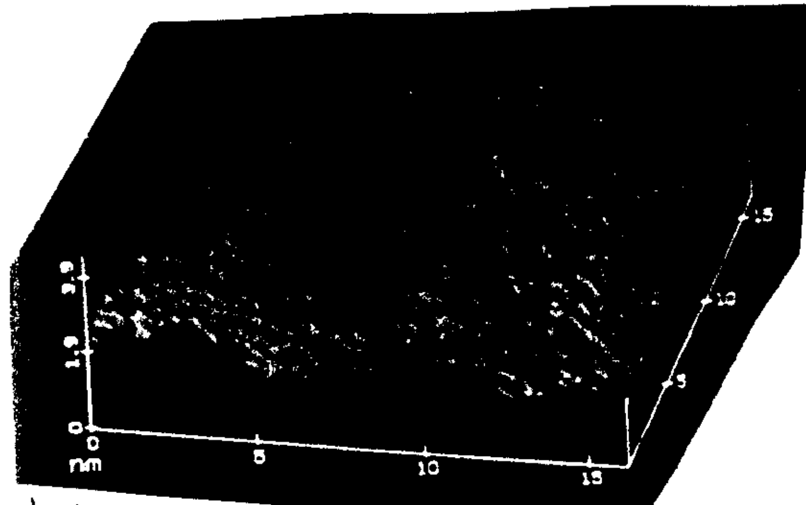


J. Krim, O. Solina & R. Chiarello PRL 66, 181 (1991)
"Ag test sample": 15 nm

J. Krim, I. Heyvaert, C. Van Haesendonck & Y. Bruynseraede, (preprint)

Ar-bombarded Iron: 100 nm

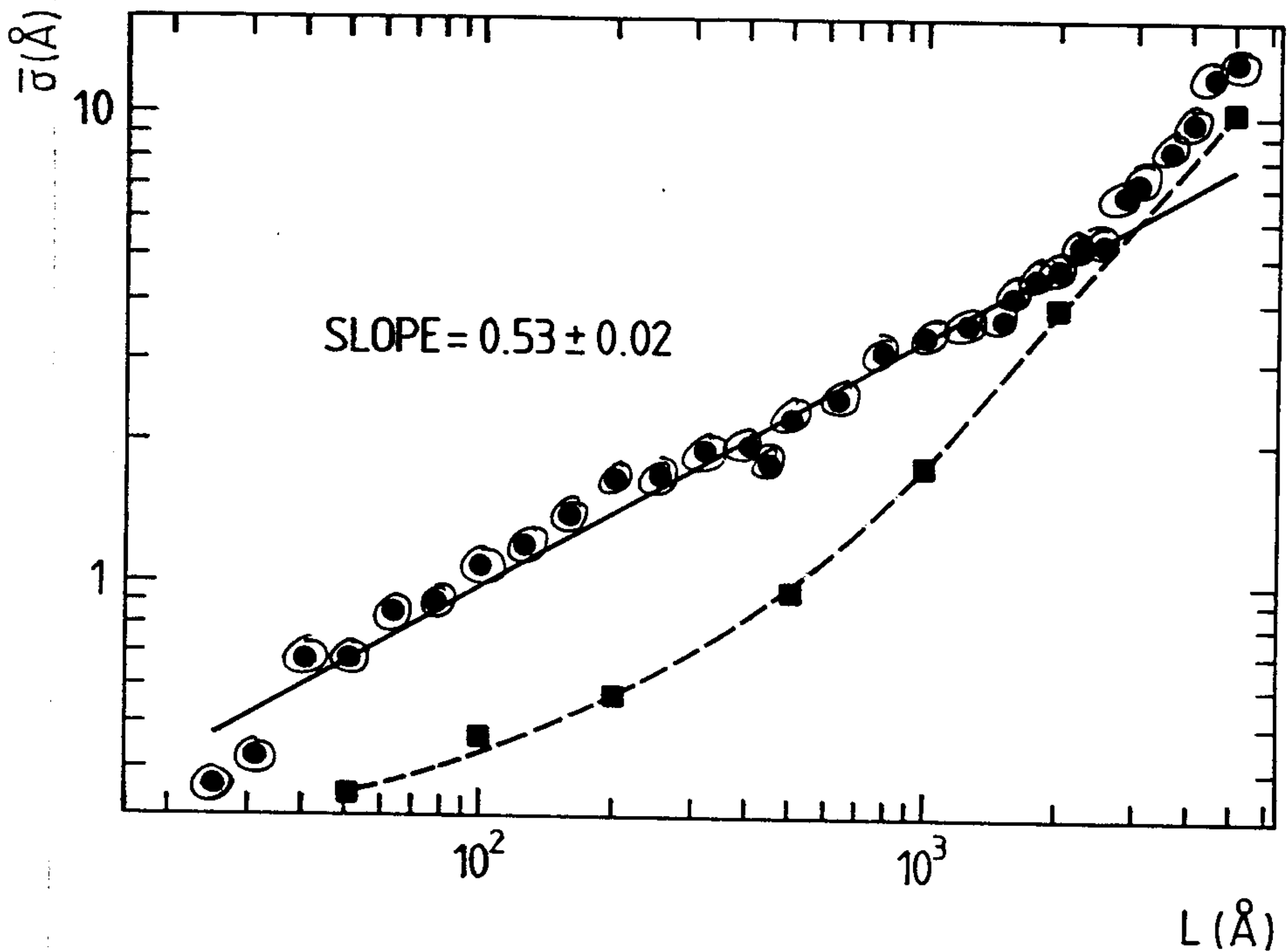


STM data for Fe film sample .... Fe(001)/MgO(001)

After annealing ... not fractal
(Stay tuned for discussions of equilibrium roughening.

After Ar-ion erosion .... $H = 0.53 \pm 0.02$
(Stay tuned for discussion of erosion)
($D = 2.47$)

5 keV $Ar^+$ ions, flux ~ $5 \times 10^{14}$ ions/cm²/s

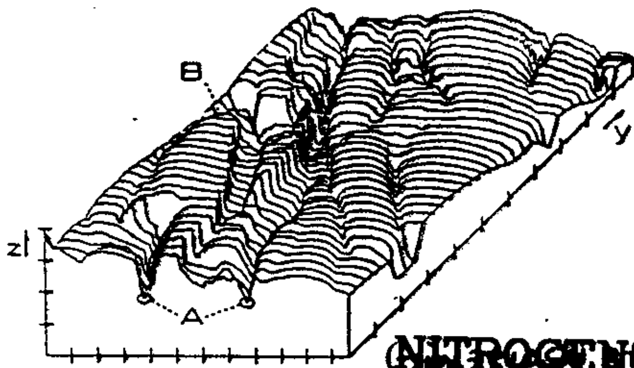


FIG. 2. An STM picture of a cold-condensed pyridine-treated Ag surface after annealing to 300 K. A, narrow trench sites where tip penetration limits topographic reproduction; B, trench sites where the tip tunnels with the bottom of the trench. Divisions on the axes correspond to 5 nm.

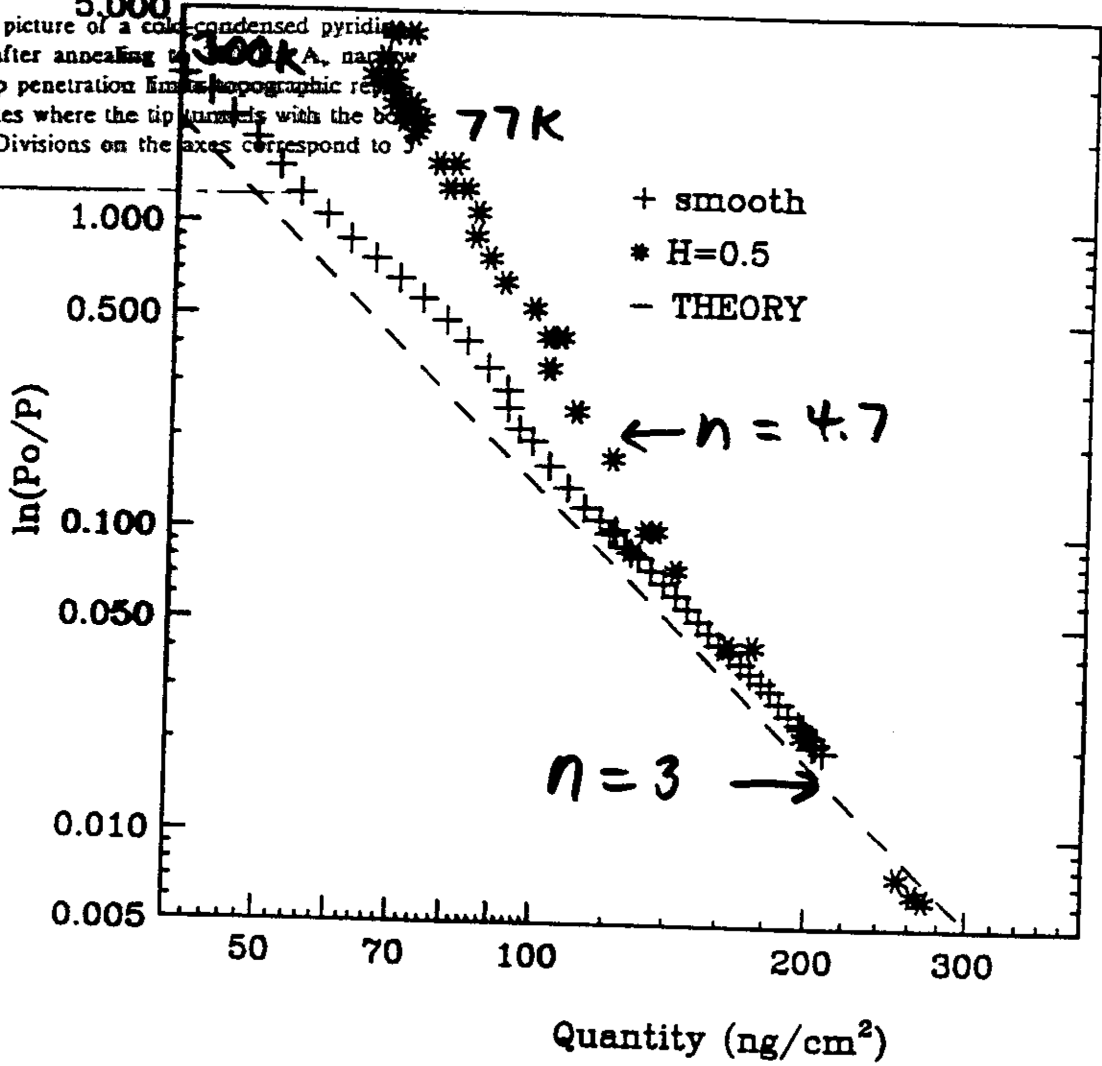


Panella & Krim PRE '94

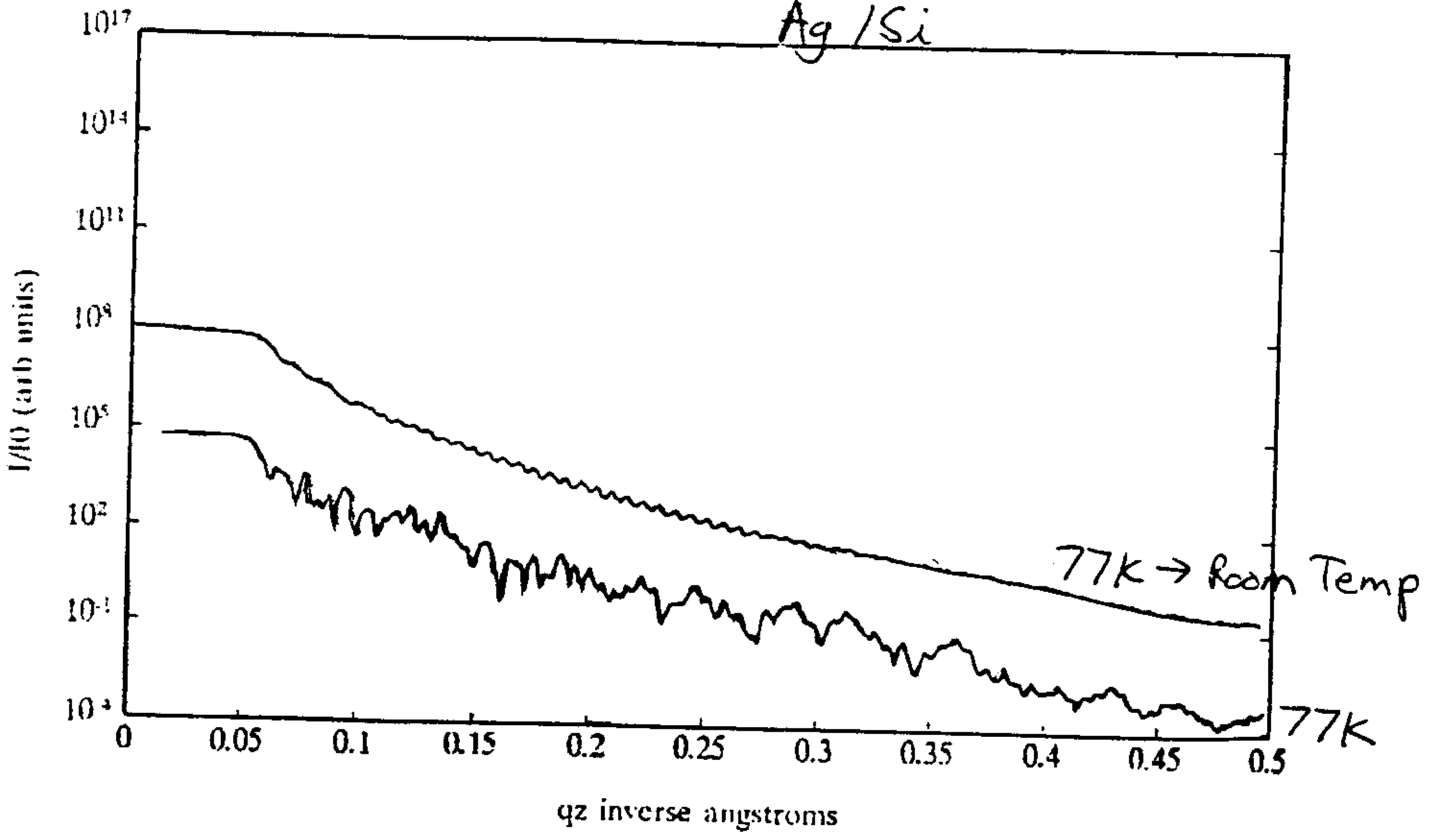
SPECULAR REFLECTIVITY
Ag /Si
I/I0 (arb units)
qz inverse angstroms
77K → Room Temp
77K
0
0.05
0.1
0.15
0.2
0.25
0.3
0.35
0.4
0.45
0.5

# Ag / quartz @77K $H \approx .5$

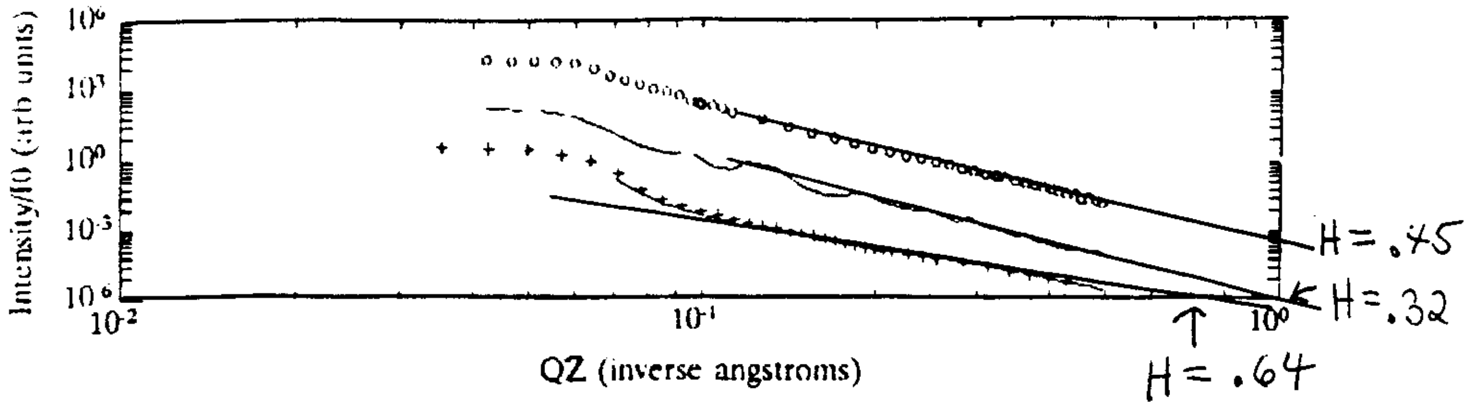


$$\text{slope} = 3 + \frac{1}{H}$$

warning!! single interface assumption!!

C. Thompson et. al. PRB '94

Chiarello et. al. PRL '91

Panella & Krim PRE '94

(c)

# Lecture III Summary

Kinetic Roughening is frequently observed in a very wide range of systems. The vast majority exhibit.

$H = .7 - 1$ and $\beta = .2 - .4$

Why? That's probably the easiest topology to observe!

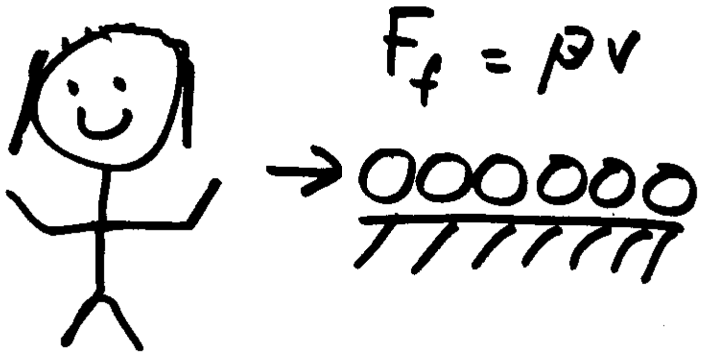
$F_f = \beta v$